Optimisation of screw anchor lateral capacity in sand for offshore renewable energy applications

Cerfontaine, Benjamin; Brown, Michael; Knappett, Jonathan; Davidson, Craig; Sharif, Yaseen

Published in:
Proceedings of the 4th International Symposium on Frontiers in Offshore Geotechnics

Publication date:
2020

Document Version
Peer reviewed version

Cerfontaine, B., Brown, M., Knappett, J., Davidson, C., & Sharif, Y. (2020). Optimisation of screw anchor lateral capacity in sand for offshore renewable energy applications. In Proceedings of the 4th International Symposium on Frontiers in Offshore Geotechnics [3451] Deep Foundations Institute. Deep Foundations Institute website: http://www.dfi.org/pubdetail.asp?id=3451

OPTIMISATION OF SCREW ANCHOR LATERAL CAPACITY IN SAND FOR OFFSHORE RENEWABLE ENERGY APPLICATIONS

B. Cerfontaine, University of Dundee, Dundee, UK, B.Cerfontaine@dundee.ac.uk
M.J. Brown, University of Dundee, Dundee, UK, M.J.Z.Brown@dundee.ac.uk
J.A. Knappett, University of Dundee, Dundee, UK, J.A.Knappett@dundee.ac.uk
C. Davidson, University of Dundee, Dundee, UK, C.S.Davidson@dundee.ac.uk
Y. Sharif, University of Dundee, Dundee, UK, Y.U.Sharif@dundee.ac.uk

ABSTRACT

Screw piles or screw anchors are a promising solution to anchor floating offshore renewable energy devices, such as wind turbines or tidal turbines. The installation generates limited noise (driven piles are noisy) and can be undertaken in all soil conditions. Although they are mainly used for their large uplift capacities, screw anchors can also be designed to provide significant lateral resistance. The optimisation of screw anchor design does not rely only on the geotechnical assessment of the uplift capacity based on soil strength, but also on operational (installation requirements) and structural (helix bending, core section stress, limiting steel plate thickness) constraints. This paper develops a methodology for the design optimisation of screw anchors under lateral loading in dense sand, incorporating all of these constraints, based on simplified analytical or semi-analytical approaches. The results show that it is possible to optimise the anchor design, maximising the anchor lateral capacity, whilst minimising the anchor weight. The maximum embedment depth and then the anchor capacity is mainly limited by the maximum torque available during installation and the short-pile to long-pile failure mechanism transition respectively.

Keywords: Geotechnical Design, Screw anchor, Offshore renewable energy, Foundation design, Anchors

INTRODUCTION

Whilst bottom-fixed foundations represent the large majority of installed offshore wind turbines, there is a huge potential for floating platform development in the EU (Wind Europe, 2018) as water depths increase. Similarly, floating tidal and wave energy converter technologies are also gaining momentum (Greaves *et al.*, 2018). As the anchoring and mooring cost of these technologies can represent a significant amount of the total capital investment, there is a need for the development of cost-efficient and innovative anchoring techniques.

Screw anchors are an onshore technology that has recently received more attention as possible alternative foundations for offshore structures generating large tensile loads (Byrne *et al.*, 2015; Davidson *et al.*, 2019). Screw anchors consists of one or several steel helices attached to a shaft and are installed by applying a torque at their top, forcing their penetration into the ground (T. Al-Baghdadi *et al.*, 2017). The installation of screw anchors generates only a limited amount of noise and vibration, which makes them environmentally and marine mammal friendly where the limitations for such noise can be very severe for pile driving (Koschinski *et al.*, 2013). These environmental constraints are more and more recognised by the offshore industry and led to the development of silent-piling methods (Huisman *et al.*, 2020).

Screw anchors are mostly used for their large uplift capacities. However, the screw anchors can simply be used as a technique to install a normal pile into the ground without noise. In this case, the role of the helix is limited to enable the pile installation, rather than to enhance its capacity. Indeed, while suction anchors can be very efficient, the success of their installation can be very dependent on the soil conditions. The lateral capacity of screw anchors becomes

of interest when they are connected to taut-lines or catenary mooring systems. While piles and suction caissons have been widely investigated before, there is no specific design methodology related to screw anchors under lateral loading for offshore applications.
The optimisation of screw anchor geometry cannot be based only on the calculation of their geotechnical lateral capacity. Indeed, the installation process is such that the capacity of installation tools (e.g. maximum torque that can be applied) and structural constraints (e.g. helix bending) limit the maximum pile diameter and installation depths that are achievable. This in turn limits the anchor lateral capacity which is only slightly affected by the helix (Al-Baghdadi *et al.*, 2015). This paper proposes to combine simplified models for the installation requirements, the structural resistance and the geotechnical capacity, to identify the optial geometry that maximises the anchor's lateral capacity while minimising its weight (or pile material utilised), as a function of the installation torque available.

METHODOLOGY

In the following, simplified models are defined to calculate the different geotechnical and structural constraints during installation or operation of the anchor.

Screw anchor geometry

The geometry of the screw anchor that will be optimised can be described as a function of a limited number of parameters, depicted in Fig. 1. It is composed of a helix of diameter D_h and pitch p_h, attached to a core of length L and diameter D_c. The pile shaft length is assumed to be equal to the embedment depth of the helix (measured at mid pitch). The core and helix thicknesses are equal to t_c and t_h respectively. The helix pitch was considered constant and equal to $D_h/3$, which lies within the range of typical geometries [0.15 D_h – 0.33 D_h] as summarised in Cerfontaine *et al.* (2019). The tip of the screw anchor is assumed to be flat.

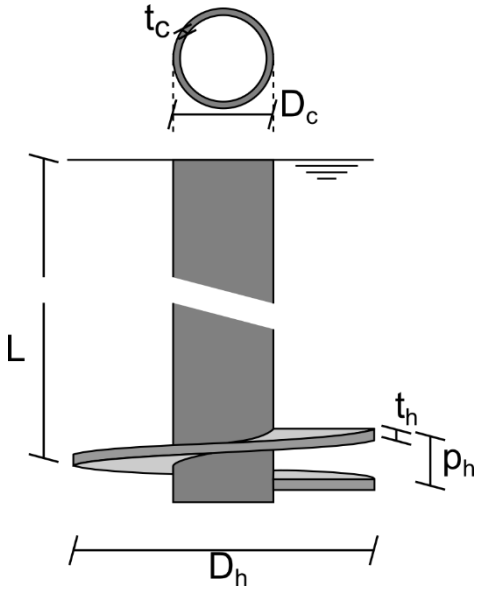

Fig. 1 Geometry of the screw anchor and definition of the main variables (Note the width to length ratio is exaggerated in this figure)

Installation Torque and vertical force

Screw piles are installed by applying a torque and possibly some vertical force at their head. These actions are necessary to overcome the shear stresses developing along the shaft, the helix and on the pile base. Some methods have been introduced in the literature to predict the installation torque and force required during installation (Davidson *et al.*, 2018). The underlying hypothesis is that the installation of the screw anchors is pitch-matched, i.e. the anchor follows a true helical movement during installation, as recommended in the literature (Perko, 2009).
The installation prediction method by Davidson et al.(2018) decomposed the development of the total torque (T) with installation depth (L) into several components related to the core (T_c), the base (T_b) and the helix (T_h) which are function of the CPT data ($\bar{q}_c$), soil parameters (δ_{crit}, K_0) and pile geometry (D_h, D_c, t_h).

$$\mathrm{T(L)} = T_c(D_c^2, \bar{q}_c(L), \delta_{crit}, L) + T_b(D_c^3, \bar{q}_c(L), \delta_{crit}) + T_h\left(D_h^3, D_c^3, \bar{q}_c(L), \delta_{crit}, t_h, K_0\right) \leq T_{max} \quad [1]$$

where $\bar{q}_c(L)$ is the averaged cone resistance q_c over $L \pm 1.5D_h$, δ_{crit} is the critical sand-steel anchor interface friction angle and K_0 is the coefficient of lateral earth pressure at rest,

calculated based on the critical state friction angle (ϕ_{crit}). A stress drop index *a* (= $F_r / \tan \delta_{crit}$), as defined by Lehane *et al.* (2005), is used in this procedure to calculate the lateral stress acting on the pile core. F_r is the CPT friction ratio, taken as equal to 0.01 in this paper. A similar method was developed to assess the vertical force (F_c) necessary to install the screw anchor while respecting the pitch-matched assumption (Al-Baghdadi, 2018).
The torque that can be applied to install the pile is limited by the equipment used and should be minimised. The torque resistance depends non-linearly on the core diameter (D_c) and the embedment depth (L). However, reducing these two geometric parameters will also reduce the lateral capacity, hence the necessary optimisation process.

Core section structural requirements

The core section is subjected to a combined torque and compressive force generated during the installation and predicted according to the methodology introduced in the previous section. The shear stress (τ) due to the torque (T) applied to the cylindrical core can be calculated according to the following equation. It is maximum at the top of the pile.

$$\tau = 16 \frac{T}{\pi} \frac{D_c}{D_c^4 - (D_c - 2t_c)^4} \quad [2]$$

Similarly, the normal stress within the core section due to the compression force applied during the installation ($F_{y,c}$) can be calculated according to

$$\sigma_y = \frac{4}{\pi} \frac{F_{y,c}}{(D_c^2 - (D_c - 2t_c)^2)} \quad [3]$$

It must be ensured that the equivalent Von Mises stress ($\sigma_{eq,c}$) is lower than the yield limit of the steel (f_y) within the core section. This equation consists of the first structural constraint.

$$\sigma_{eq,c} = \sqrt{\sigma_y^2 + 3\tau^2} \leq f_y \quad [4]$$

In addition, the compressive force can be very large, inducing a risk of buckling of the pile, which is only partly restrained by the surrounding soil. A simplified approach consists of calculating the first mode of elastic buckling according to the Euler equation. A very conservative approach was adopted, considering that the pile tip was clamped ($K = 2$), due to helix restraint on the rotation at the anchor tip, and the pile top was free to move laterally and rotate. Consequently, the second structural constraint states that the elastic buckling force ($F_{y,cr}$) must be always larger than the compression force ($F_{y,c}$) necessary during the installation.

$$F_{y,cr}(HL) = \pi^2 \frac{EI}{(\mathrm{KL})^2} \geq F_{y,c}(L). \quad [5]$$

Finally, a purely geometrical constraint was added on the maximum core thickness (t_c) that is practically possible to manufacture. It was assumed that t_c was lower than 10% of the core diameter D_c and never larger than 100mm. This is in accordance with thick pile dimensions that were found in manufacturer's catalogues, (e.g. JFE, 2019). To simplify the comparison between the different anchor geometries, the relative core thickness $t_{c,rel}$ was introduced such that

$$t_{c,rel} = \frac{t_c - t_{c,min}}{t_{c,max} - t_{c,min}}. \quad [6]$$

Helix failure

The helix is necessary for the pile installation process, as it may assist pile penetration if an appropriate advancement ratio is adopted (Huisman *et al.*, 2020). A significant load may act upon the helix during the installation process or pile loading. Therefore failure of the helix can be caused by yielding of the helix plate (Fig. 2(b)) or failure of the welded connection with the core (Fig. 2(c)).
The helix herein was idealised as a flat plate clamped to the central core with a full moment fixity, that can be achieved through welding as shown in Fig. 2(a). The maximum horizontal stress within the helix (σ_x) is calculated based on the approach proposed by Timoshenko and Woinowky-Krieger (1959) to calculate bending stresses in plates. This analytical model assumes that the pressure applied onto the helix is constant and that the helix is a horizontal annular plate, as discussed in (Cerfontaine *et al.*,2020). The horizontal stress is then calculated as

$$\sigma_x = k\frac{qD_h^2}{4t_h^2} \leq f_y \qquad [7]$$

where *k* is a constant depending on the D_h/D_c ratio, given in Table 1 and *q* is the maximum normal stress applied to the helix (during installation or pile loading). The normal force acting on the helix during the installation can be calculated directly from the CPT prediction method (equation similar to Eq. [1]) or is equal to the uplift capacity during pile loading (see hereafter). The normal stress acting on the helix (*q*) is simply obtained by dividing this normal force by the helix surface area. The helix plate thickness (t_h) was considered to be equal to a maximum of 100mm at the connection. The helix bending constraint ensures that the maximum horizontal stress within the plate σ_x is no greater than f_y.

Table 1 Coefficient k as a function of D_h/D_c, (Timoshenko *et al.*, 1959)

D_h/D_c [-]	1.25	1.5	2	3	4
k [-]	0.135	0.410	1.04	2.15	2.99

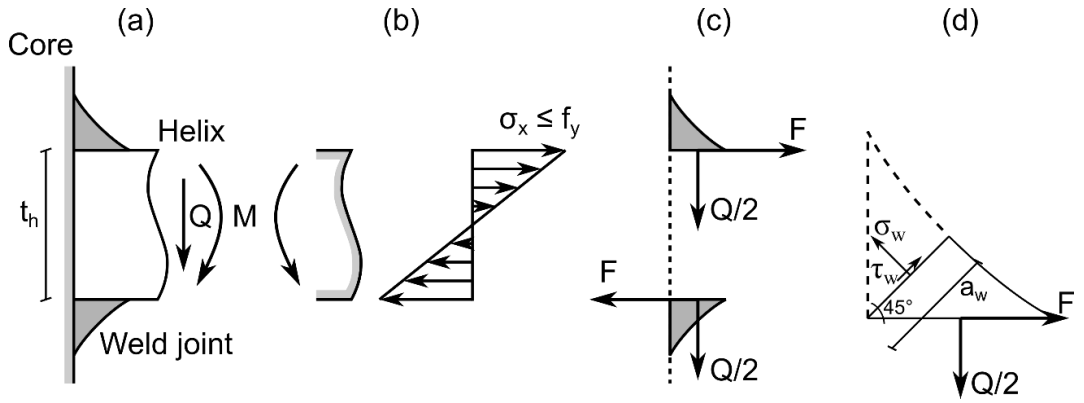

Fig. 2 Idealisation of the connection between the helix and the core: (a) Bending moment and shear load Q; (b) Horizontal stress due to helix bending; (c) Loads acting on the weld joints; (d) Stress state along the weld throat a_w

Lateral Capacity

Contrary to suction caissons or driven piles, the screw-in installation method of screw anchors requires that the mooring line is likely to be attached at the head of the pile. The maximum capacity of the anchor was calculated based on the methodology detailed in Randolph and Gourvenec, (2011). The passive earth pressure within the soil will be mobilised by its lateral displacement. Short and long pile mechanisms can be identified, as shown in Fig. 3. For short piles, the failure is due to full mobilisation of the soil capacity. For long piles, a plastic hinge is formed when the pile core section yields. It was shown that the pull-out load applied to the helix has only a limited effect on the lateral capacity (Al-Baghdadi *et al.*, 2017), therefore it was decided to neglect this coupling in this simplified approach.

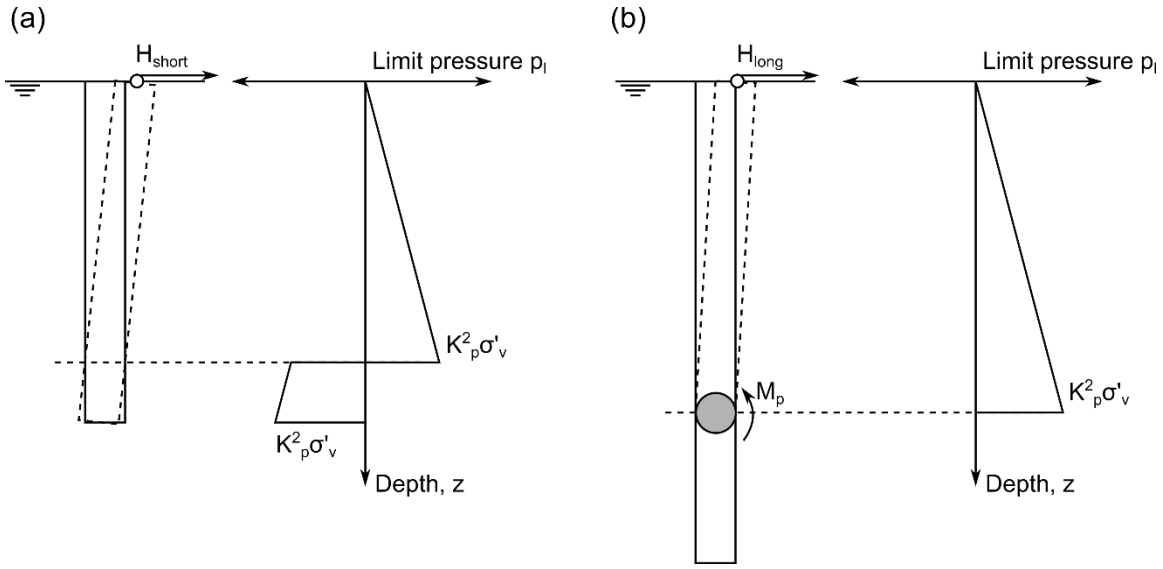

Fig. 3 Calculation of the maximum lateral load (H) as a function of a short (a) or long (b) pile failure mechanism, after (Randolph *et al.*, 2011)

An analytical solution can be found to calculate the horizontal load corresponding to each mechanism (H_{short} or H_{long}) in a non-dimensional form.

$$\frac{H_{short}}{K_P^2 \gamma' D_c^3} = \left(\frac{L}{D_c}\right)^2 (0.5^{\frac{2}{3}} - 0.5) \quad [8]$$

$$\frac{H_{long}}{K_P^2 \gamma' D_c^3} = 0.5\,(3\mu_p)^{\frac{2}{3}} \quad [9]$$

where K_p is coefficient of passive earth pressure and $\mu_p = M_p/(K_p^2 \gamma' D_c^4)$. The plastic moment M_p is a function of the core section properties.

$$M_p = \frac{4}{3} f_y D_c^3 \left[\left(\frac{t_c}{D_c}\right)^3 - \frac{3}{2}\left(\frac{t_c}{D_c}\right)^2 + \frac{3}{4}\left(\frac{t_c}{D_c}\right)\right] \quad [10]$$

This non-dimensional solution shows in Fig. 4 that the lateral capacity increases non-linearly with depth (short-pile solution) and is bounded by the long-pile capacity. Subsequently, the maximum embedment depth will be limited to the transition from short- to long-pile failure mode.

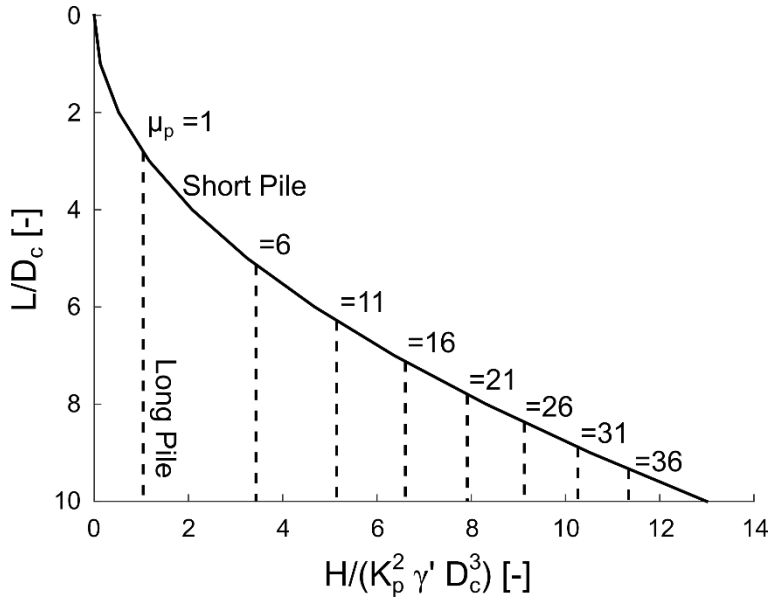

Fig. 4 Non-dimensional lateral capacity of a pile as a function of depth and non-dimensional properties of the core section (μ_p)

Vertical capacity

The vertical capacity of the anchor can be calculated according to the method proposed by Giampa *et al.*, 2017. As the vertical capacity is not used in the optimisation algorithm, the equations are not repeated here. In this case, it is assumed that the failure mechanism in uplift forms a truncated wedge, whose inclination to the vertical is equal to the dilatancy angle and initiating from the helix. It is assumed that the maximum relative embedment depth (L/D_h) at which this capacity can be achieved is limited to 8 to ensure a shallow failure mechanism forms, rather than a flow around deep failure mechanism (Meyerhof *et al.*, 1968).

RESULTS

The optimisation consists in calculating the maximum depth L (and then capacity H) that can be reached for a given screw anchor geometry (D_c, D_h/D_c =2, t_c) in a given soil. Different scenarios are assumed regarding the maximum torque available during installation (T_{max}, varying between 1MNm and 15MNm). The maximum depth will be limited by the different constraints previously described. For each configuration, it is possible to identify the anchor geometry maximising the lateral capacity while minimising the anchor weight. The results do not include any factor of safety, as they vary country by country. A suitable value can be applied to the anchor resistance as a whole (DNV-GL, 2018), once calculated.

Soil and screw anchor properties

The soil conditions considered here correspond to a homogeneous layer of dense HST95 test sand (D_r = 82%). The properties of the sand were previously determined by Al-Defae *et al.* (2013). The peak strength properties (friction angle ϕ_p and dilatancy angle ψ_p), the critical state friction angle ϕ_{crit}, the soil-steel critical friction angle δ_{crit} and the buoyant unit weight γ' used are reported in Table 2. A CPT test was undertaken in-flight in a beam centrifuge at the University of Dundee (Davidson *et al.*, 2018) and served as an input to predict the installation requirements. The steel yield limit f_y was assumed to be 350MPa.

Table 2 Properties of the HST95 sand (D_r = 82%)

ϕ_p [°]	ϕ_{crit} [°]	ψ_p [°]	δ_{crit} [°]	γ' [kN/m³]
45.4	32	16.5	24	10.47

Determination of the maximum embedment depth for a given geometry

The different geotechnical and structural constraints are graphically represented in Fig. 5 for a configuration characterised by: D_c=0.85m, D_h/D_c = 2, $t_{c,rel}$ =0.1. The maximum depth is given as L_{max} and corresponds to the short to long pile transition constraint, as shown in Fig. 5(b). The torque (T) and force (F_c) installation requirements are given in Fig. 5(a) and (b) respectively. In this case, the torque is lower than the maximum (assumed equal to 5MNm) and the vertical force is lower than the critical buckling load. Similarly, the stress in the helix and the core is lower than the yield strength (Fig. 5(c)). The maximum depth is then equal to 6.1m and the horizontal capacity is equal to 1.53MN for this configuration.

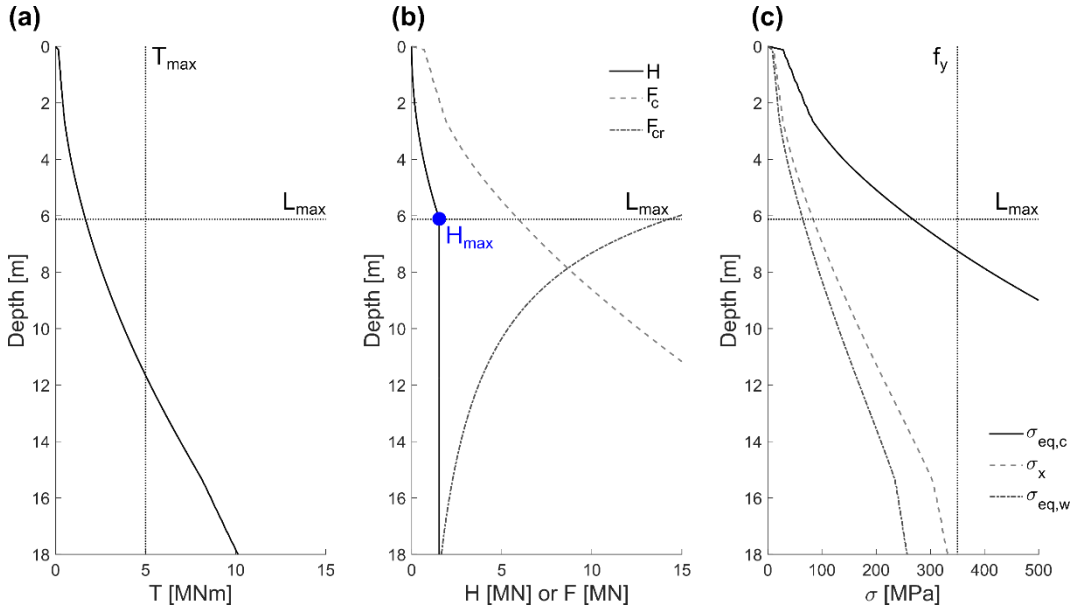

Fig. 5 Determination of the maximum embedment depth based on different geotechnical and structural constraints for a screw pile of a given geometry (D_c = 0.85m, D_h/D_c =2, $t_{c,rel}$ =0.1) and maximum torque available T_{max} = 5MNm.

Optimisation as a function of the core thickness

The same procedure can be repeated over a large number of different configurations, varying the core section diameter (D_c) and the core thickness ($t_{c,rel}$),while maintaining a constant maximum torque available (T_{max}). For each case, the maximum embedment depth and the lateral capacity can be calculated. They are limited by one of the constraints such as the maximum torque available or an insufficient pile section to sustain the installation torque. An example is presented in Fig. 6 which assumes a maximum torque available for installation equal to 5MNm and D_h/D_c equal to 2.

Fig. 6(a) shows the evolution of the lateral capacity (H) as a function of the pile core diameter (D_c) and the relative core thickness ($t_{c,rel}$). The maximum pile length associated with the capacity is reported in Fig. 6(b). For a given relative core thickness ($t_{c,rel}$), the embedment depth achievable (L) and the lateral capacity (H) both increase with the core diameter (D_c). At low core diameters, the depth and capacity are limited by the short to long pile failure mode. In other words, increasing the depth will not result in an increase of lateral capacity. At larger core diameters, the depth is limited because the torque available is insufficient to install the pile to a greater depth. In other words, a larger capacity would be possible from a geotechnical point of view, but it would be practically impossible to reach it. Finally, if the relative core thickness is too low, the capacity of the section to sustain the installation torque may become the limiting constraint.

It is obvious that the largest relative core wall thickness will always lead to the largest capacity for a given core diameter. However, if the horizontal capacity (H) is traced as a function of the

weight of the anchor, it is apparent that this is not an efficient design, as shown in Fig. 6(b). This figure depicts the evolution of the anchor capacity as a function of the weight (as an analogue to material use and handling requirements). The thickest anchor wall is only efficient if the necessary lateral capacity lies between 4.5 and 5MN, otherwise a lighter anchor would provide the same capacity with a lower amount of steel. An envelope representing the evolution of the lateral capacity as a function of the anchor weight can then be traced and is only a function of the maximum torque available. Finally, the vertical capacity corresponding to the installation depth is also calculated and is given in Fig. 6(d) for information. In this figure, it is assumed that there is no interaction between the lateral and vertical capacity, but more research is needed to quantify the probable interaction.

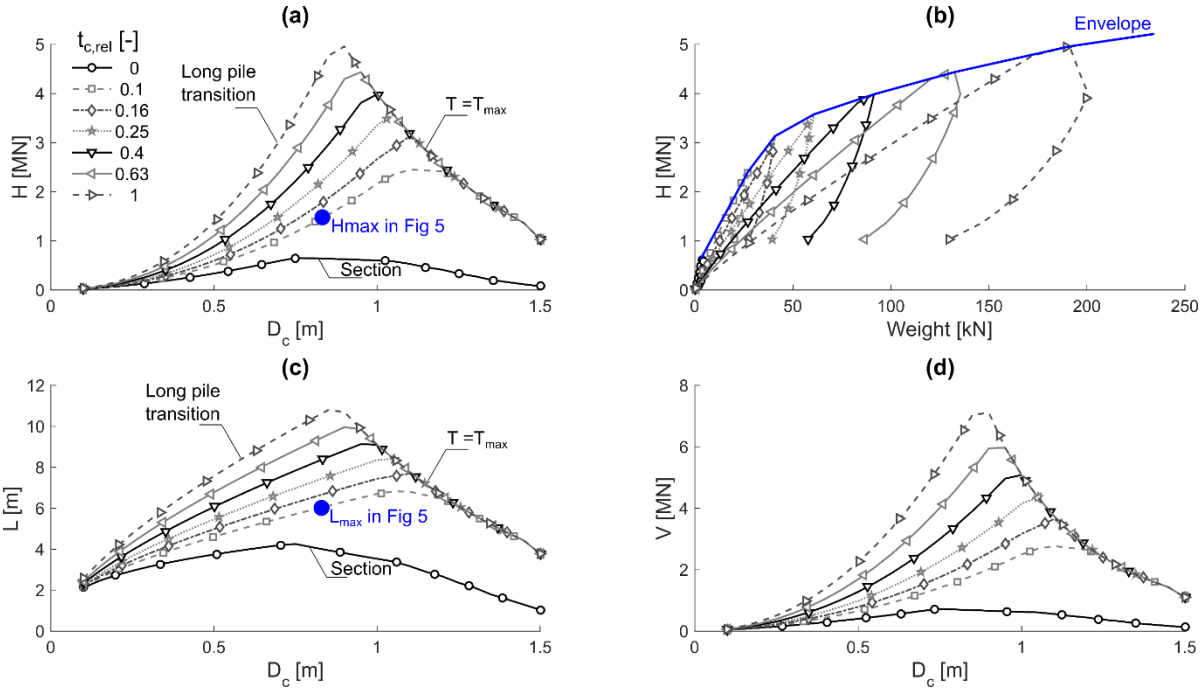

Fig. 6 Results of the calculation procedure for a screw pile (D_h/D_c=2) and a maximum torque available (T_{max}) equal to 5MNm.

Optimisation with respect to maximum weight

The envelope obtained in the previous section can be calculated for each maximum torque available. These envelopes are gathered into a single final design chart, given in Fig. 7. It shows that the gain in capacity achieved by increasing the maximum torque is much larger from 1MNm to 7MNm, than from 7MNm to 15MNm. Larger capacities are obtained through the installation of larger diameter anchors, which in turn necessitate a much larger torque to be installed. The gain in depth/capacity is limited by the strength and buckling of the core section.

Improvements of the design optimisation methodology

The purpose of this paper is to illustrate how structural and geotechnical parameters affect the design of screw piles. It is based upon simplified hypotheses and all components of the design can be improved or refined independently. The CPT prediction method has been validated only against uniform sand materials to date, but non-homogeneous sand conditions can be directly incorporated through the CPT data. The prediction of the lateral capacity can be enhanced similarly, for instance by using depth-dependent p-y curves to calculate the pile capacity coupled with a limiting displacement criterion. Such a framework can also include cyclic loading effects, which are not included here but could be predicted through empirical relationships developed for piles (Richards *et al.*, 2019).

Some other improvements of the method will require additional research before simplified models can be derived. For instance, the couplings between vertical and lateral loading (for taut-line applications) cannot be predicted yet. Geometrical effects (e.g. the pile tip shape) and installation parameters (overflighting rather than pitch-matched installation, (Huisman *et al.*, 2020)) still have to be studied and implemented in the CPT prediction method.

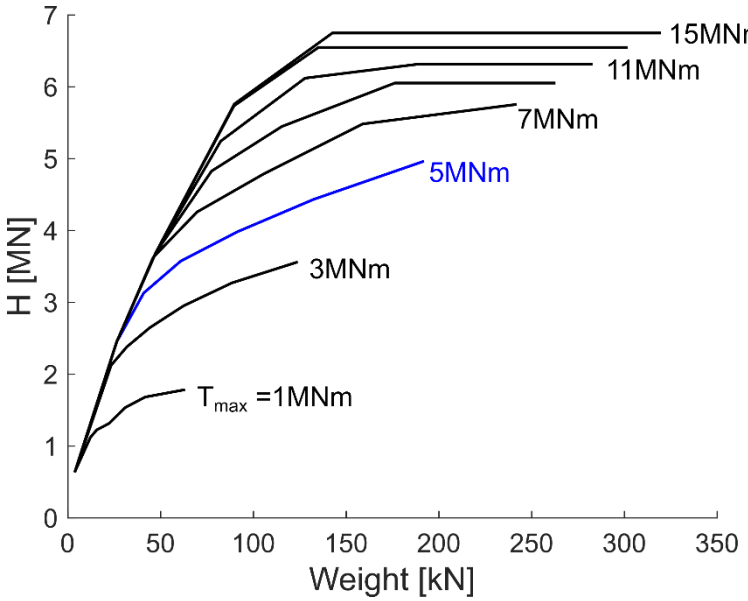

Fig. 7 Summary of envelopes of the lateral capacity (h) as a function of the anchor weight. Each envelope corresponds to a maximum torque available for a screw anchor (D_h/D_c =2). The blue curve is the envelope determined in Fig. 6(b).

SUMMARY AND CONCLUSIONS

It has been shown that the design of screw anchors depends on both structural (core strength, helix strength) and geotechnical (capacity, installation requirements) constraints, which must all be assessed prior to installation and operation. These constraints limit the maximum embedment depth of the anchor and the resulting horizontal capacity.
All of these constraints can be assessed by combining simplified analytical methods. It is therefore possible to calculate the maximum embedment depth for a given anchor geometry and then its capacity. The optimum design, namely the largest capacity achieved for a minimum weight, can be calculated as a function of the maximum torque available during the installation. A design chart is provided to quickly assess the optimum capacity in a dense layer of sand.

ACKNOWLEDGEMENTS

This project has received funding from the European Union's Horizon 2020 research and innovation programme under the Marie Skłodowska-Curie grant agreement No 753156. The authors would also like to acknowledge the support of EPSRC (Grant no. EP/N006054/1: Supergen Wind Hub: Grand Challenges Project: Screw piles for wind energy foundations)

REFERENCES

Al-Baghdadi, T. *et al.* (2017) 'CPT-Based Design Procedure for Installation Torque Prediction for Screw Piles Installed in Sand', *Offshore Site Investigation Geotechnics 8th International Conference Proceedings*, (1), pp. 346–353. doi: 10.3723/osig17.346.
Al-Baghdadi, T. (2018) *Screw piles as offshore foundations : Numerical and physical modelling*. PhD Thesis, University of Dundee, UK.

Al-Baghdadi, T. A. *et al.* (2015) 'Modelling of laterally loaded screw piles with large helical plates in sand', in *3rd International Symposium on Frontiers in Offshore Geotechnics*. Oslo, Norway: CRC Press/Balkema, pp. 503–508.
Al-Baghdadi, T. A. *et al.* (2017) 'Geotechnical engineering effects of vertical loading on lateral screw pile performance', *Proceedings of the Institution of Civil Engineers: Geotechnical Engineering*, 170(3), pp. 259–272. doi: 10.1680/jgeen.16.00114.
Al-Defae, A. H., Caucis, K. and Knappett, J. A. (2013) 'Aftershocks and the whole-life seismic performance of granular slopes', *Geotechnique*, 63(14), pp. 1230–1244. doi: 10.1680/geot.12.P.149.
Byrne, B. W. and Houlsby, G. T. (2015) 'Helical piles: an innovative foundation design option for offshore wind turbines', *Philosophical Transactions of the Royal Society A: Mathematical, Physical & Engineering Sciences*, 373(February), pp. 1–11. doi: 10.1098/rsta.2014.0081.
Cerfontaine, B. *et al.* (2019) 'Effect of soil deformability on the failure mechanism of shallow plate or screw anchors in sand', *Computers and Geotechnics*, 109(May), pp. 34–45. doi: https://doi.org/10.1016/j.compgeo.2019.01.007.
Cerfontaine, B. *et al.* (2020) 'Optimised design of screw anchors in tension in sand for renewableenergy applications', *(submitted for publication in) Ocean Engineering*.
Davidson, C. *et al.* (2018) 'A modified CPT based installation torque prediction for large screw piles in sand', in Hicks, M., Pisanò, F., and Peuchen, J. (eds) *Cone Penetration Testing*. Delft, The Netherlands. doi: https://doi.org/10.1201/9780429505980.
Davidson, C. *et al.* (2019) *ISSPEA 2019: 1st International Symposium on Screw Piles for Energy Applications*. Dundee, Uk: University of Dundee.
DNV-GL (2018) *DNVGL-ST-0119 Floating wind turbine structures*.
Giampa, J., Bradshaw, A. and Schneider, J. (2017) 'Influence of Dilation Angle on Drained Shallow Circular Anchor Uplift Capacity', *International Journal of Geomechanics*, 17(2), p. 4016056. doi: 10.1061/(ASCE)GM.1943-5622.0000725.
Greaves, D. and Iglesias, G. (2018) *Wave and tidal energy*. John Wiley & Sons, Ltd.
Huisman, M. *et al.* (2020) 'Silent deep foundation concepts: push-in and helical piles', in *4th Int. Symp. on Frontiers in Offshore Geotechnics*. Austin, Texas.
JFE (2019) *JFE Steel corporation major building materials catalog*. Available at: http://www.jfe-steel.co.jp/en/products/list.html#! (Accessed: 16 March 2019).
Koschinski, S. and Lüdemann, K. (2013) 'Development of Noise Mitigation Measures in Offshore Wind Farm Construction 2013', *Report commissioned by the Federal Agency for Nature Conservation (Germany)*, (February), p. 102 pp. Available at: http://mhk.pnl.gov/publications/development-noise-mitigation-measures-offshore-wind-farm-construction.
Lehane, B., Schneider, J. and Xu, X. (2005) 'The UWA-05 method for prediction of axial capacity of driven piles in sand', in Gourvenec, S. and Cassidy, M. (eds) *Frontiers in Offshore Geotechnics: ISFOG*. Perth, Asutralia, pp. 683–689. doi: 10.1201/noe0415390637.ch76.
Meyerhof, G. G. and Adams, J. I. (1968) 'The ultimate uplift capacity of foundations', *Canadian Geotechnical Journal*, 5(4), pp. 225–244.
Perko, H. A. (2009) *Helical Piles: A Practical Guide to Design and Installation*. 1st Edit. John Wiley & Sons. doi: 10.1002/9780470549063.
Randolph, M. and Gourvenec, S. (2011) *Offshore Geotechnical Engineering*. 1st Edit. London: CRC Press.
Richards, I. A., Byrne, B. W. and Houlsby, G. T. (2019) 'Monopile rotation under complex cyclic lateral loading in sand', *Géotechnique*, pp. 1–15. doi: 10.1680/jgeot.18.p.302.
Timoshenko, S. and Woinowky-Krieger, S. (1959) *Theory of Plates and Shells*. 2nd Edit. McGraw-hill.
Wind Europe (2018) *Technical report: Offshore Wind in Europe, key trends and statistics*.